Effect of Limiters on Higher Order Computation of Shock Tube Problem

Mohammad Asif Sultan, Manash Jyoti Konwar

Abstract— In this paper, some Computational Fluid Dynamics (CFD) techniques have been used to compute the variations in different parameters like pressure, density etc. by solving the Euler Equations for shock tube problem. The governing equations are discretized on a Finite Volume framework. Van Leer's first, second and third order flux vector splitting method have been used to compute the inviscid flux terms. For the second order computations, MUSCL approach has been adopted. The effect of the order of the scheme on the accuracy of the solution is studied. Also for higher order schemes the effect of the limiter type on the performance of the scheme are investigated. The performance of the scheme is judged by its ability to resolve shocks, expansion fans and contact discontinuities present in the shock tube problem. Two types of limiters namely Minmod limiter and Van Albada limiter are used for the implementation of MUSCL scheme. Van Albada limiter is found to be more robust and accurate as compared to Minmod limiter.

Index Terms - Compressible Flow, Inviscid flow, Shock waves, Flux Vector Splitting, MUSCL scheme and Conservation laws

1 INTRODUCTION

The flow of an inviscid gas is governed by the Euler Equations. Additionally the equation of state relates the different properties by some functional relationship. In the present work, the flow through a shock tube problem is analyzed

The time evolution of this problem can be described by solving the Euler equations which leads to three characteristics, describing the propagation speed of the various regions of the system namely the rarefaction wave, the contact discontinuity and the shock discontinuity. If this is solved numerically, one can test against the analytical solution, and get information how well a code captures and resolves shocks and contact discontinuities and reproduce the correct density profile of the rarefaction wave.

A compressible flow-field [3] is often characterized by the presence of discontinuities in the form of shock waves, contact discontinuities and other types of waves and wave interactions like expansion waves, shock-expansion interaction, shock-shock interaction etc. Over years, different numerical schemes are being developed for more accurate and efficient capturing of shocks. As the derivatives of the flow variables become undefined at discontinuities, so in the numerical schemes for capturing shocks, some numerical dissipation or artificial dissipation was intentionally induced so as to convert these regions of discontinuities into zones of very sharp gradients, thereby allowing obtaining of weak solutions of the governing solutions.

The first notable approach to numerical shock capturing through numerical dissipation was presented by von Neumann et.al. A numerical dissipation [4] term was introduced which assumed relatively high values near shocks and became small in smooth regions of flow. Followed by this many researchers continued work in characterization and designing of numerical dissipation.

Sod [6] provided a survey of different numerical schemes for solving system of hyperbolic conservation laws. Many different numerical schemes were tested on a 1-D shock tube problem and the results were analyzed.

Knight [4] focuses on the unsteady one dimensional Euler equations, which form the basis for development of numerical algorithms in compressible fluid mechanics. A higher order reconstruction technique such as the MUSCL is extensively discussed. The MUSCL approach was adopted in the numerical schemes.

Roe [9] presented his well-known scheme which started an era of so-called Flux-Difference-Splitting (FDS) Schemes for inviscid compressible flows. In Roe's scheme, the numerical dissipation was found suitable for capturing shocks and provided relatively lesser numerical dissipation in the smooth regions of flow. However, computational complexity was more. The quests for simpler schemes lead to the Flux Vector Splitting (FVS) Schemes. Stager and Warming [10] van Leer's flux vector splitting scheme was a noticeable step in the era of Flux Vector Splitting Schemes. Although computationally simpler as compared to the FDS, FVS had the inherent problem of more smearing of shocks and contact discontinuities due to higher numerical dissipation. Also, in viscous flows, this excessive numerical dissipation causes diffusion of boundary layers. Van Leer again suggested that better results could be obtained by blending the positive features of FVS and FDS.

Jaisankar [12, 13] showed in his paper that diffusion regulation parameter adjusts itself in different regimes of the flow and leads to the exact capturing of steady contact discontinuities which are aligned with the grid lines. This diffusion regulator parameter reduces numerical dissipation, is very

Nomenclature

ρ = Density of the Fluid.
p = Pressure of the fluid.
T = Temperature of the fluid.
R = Universal gas constant .
u, v, w =Velocities along x, y, z directions.
t = Time.
a = Velocity of Sound.
γ = Adiabatic index.
e_m = Energy per unit mass.
ϕ = Any particular property such as mass, momentum, energy per unit mass.
U = Vector of Conserved variable.
G = Flux Vector.
A = Flux Jacobian.
H =Enthalpy.
C_p =Specific heat.
U_s =Velocity of the Normal Shock.
U_p = Velocity of the Contact Surface.
M = Mach number.
V = Volume of the Cell.

simple and can be easily incorporated in any Eulerian solver. By coupling such parameters with a simple numerical method like Van Leer's Flux Vector Splitting Method, an accurate yet simple numerical method is developed for the numerical simulation of inviscid compressible flows.

Kapahi [15] described a three dimensional Eulerian and Lagrangian method for the modelling and simulation of high speed multi material dynamics. The approach showed capabilities to resolve and capture non linear waves such as shock waves, rarefaction waves and contact discontinuities in complex geometries.

It is seen that there is a continuous effort in the research field of CFD to develop more robust and efficient numerical schemes for compressible flow computations. If numerical scheme can predict approximate results as that of analytical solutions we can get information how well a code captures and resolves shocks and contact discontinuities and reproduce the correct density profile of the rarefaction wave and this can be used in solving complex fluid problems which are difficult or impossible to solve analytically. In this paper, some Computational Fluid Dynamics (CFD) techniques [1] have been used to compute the variations in different parameters like pressure, density etc. by solving the Euler Equations for the shock tube problem. The governing equations are discretized on a Finite Volume framework [2]. Van Leer's [7] first order and second order flux vector splitting method has been used to compute the inviscid flux terms. It is planned to study the effect of the order of the scheme on the accuracy of the solution. For higher order schemes the effect of the limiter type on the performance of the scheme shall also be highlighted. The performance of the scheme shall be judged by its ability to resolve shocks, expansion fans and contact discontinuities present in the shock tube problem.

2 Governing Equations

2.1 Reynolds Transport Theorem:

The Reynolds Transport Theorem (RTT) for any intensive property ϕ is given by,

$$\iiint_{system} \frac{d}{dt}(\rho\phi)\,dV = \iiint_{CV} \frac{\partial}{\partial t}(\rho\phi)\,dV + \iint_{CS} (\rho\phi)\vec{V}.\vec{dS} \qquad (1) \quad (1)$$

2.2 Continuity Equation:

For the continuity equation,

$$\phi = \frac{Mass}{Mass} = 1$$

Also, from the definition of system, when $\phi = 1$, then

$$\iiint_{system} \frac{d}{dt}(\rho\phi)\,dV = 0 \qquad (2)$$

Hence, the continuity equation, which is nothing but conservation of mass, becomes,

$$\iiint_{CV} \frac{\partial \rho}{\partial t} dV + \iint_{CS} \rho\vec{V}.\vec{dS} = 0 \qquad (3)$$

The differential form of the continuity equation, which may also be expressed as,

$$\frac{\partial \rho}{\partial t} + \frac{\partial(\rho u)}{\partial x} + \frac{\partial(\rho v)}{\partial y} + \frac{\partial(\rho w)}{\partial z} = 0 \qquad (4)$$

2.3 Momentum Equation:

The Momentum Equation is based upon Newton's Second Law of Motion, i.e.,

$$\frac{d}{dt}\iiint_{system} \rho\vec{V}dV = \left(\overrightarrow{F_{net}}\right)_{external} \qquad (6) \qquad (5)$$

Hence for Momentum Equation,

$$\phi = \frac{Momentum}{Mass} = \vec{V}$$

For Euler Equations for a gas, the external forces acting are pressure force alone, since Euler Equation is for an inviscid fluid and for gases the body forces in the form of gravity are negligible.
Hence,

$$\left(\overrightarrow{F_{net}}\right)_{external} = -\iint_{CS} p\overrightarrow{dS} \qquad (6)$$

Simplified to differential forms of the momentum equation along three mutually perpendicular directions *x*, *y* and *z* as follows,

x Momentum Equation:

$$\frac{\partial(\rho u)}{\partial t}+\frac{\partial\left(p+\rho u^2\right)}{\partial x}+\frac{\partial(\rho uv)}{\partial y}+\frac{\partial(\rho uw)}{\partial z}=0 \tag{7}$$

y Momentum Equation:

$$\frac{\partial(\rho v)}{\partial t}+\frac{\partial(\rho vu)}{\partial x}+\frac{\partial\left(p+\rho v^2\right)}{\partial y}+\frac{\partial(\rho vw)}{\partial z}=0 \tag{8}$$

z Momentum Equation:

$$\frac{\partial(\rho w)}{\partial t}+\frac{\partial(\rho wu)}{\partial x}+\frac{\partial(\rho wv)}{\partial y}+\frac{\partial\left(p+\rho w^2\right)}{\partial z}=0 \tag{9}$$

These are the differential form of the Momentum Equation for an inviscid compressible fluid.

2.4 Energy Equation:

The Energy Equation is based upon the first law of thermodynamics, which states that the total increase in Energy of a system is the sum of heat transfer into the system and the work done of the system, i.e.,

$$\frac{dE_{system}}{dt}=\frac{dQ_{system}}{dt}+\frac{dW_{system}}{dt} \tag{10}$$

Hence for the energy equation, for an inviscid compressible fluid,

$$\phi=\frac{E_{system}}{Mass}=e_m=c_vT+\frac{1}{2}\left(u^2+v^2+w^2\right) \tag{12}$$

$$or,\frac{\partial e}{\partial t}+\frac{\partial\{(p+e)u\}}{\partial x}+\frac{\partial\{(p+e)v\}}{\partial x}+\frac{\partial\{(p+e)w\}}{\partial x}=0 \tag{11}$$

is the differential form of the Energy Equation for an adiabatic inviscid compressible flow.

2.5 Euler Equations for One-Dimensional Adiabatic Flow

The Equations in the above section can be generally written as Euler Equation with the form,

$$\frac{\partial U}{\partial t}+\frac{\partial G}{\partial x}+\frac{\partial F}{\partial y}+\frac{\partial H}{\partial z}=0 \tag{12}$$

Where,

$$U=\begin{pmatrix}\rho\\ \rho u\\ \rho v\\ \rho w\\ e\end{pmatrix}\quad G=\begin{pmatrix}\rho u\\ p+\rho u^2\\ \rho vu\\ \rho wu\\ (p+e)u\end{pmatrix}\quad F=\begin{pmatrix}\rho v\\ \rho uv\\ p+\rho v^2\\ \rho wv\\ (p+e)v\end{pmatrix}\quad H=\begin{pmatrix}\rho w\\ \rho uw\\ \rho vw\\ p+\rho w^2\\ (p+e)w\end{pmatrix}$$

For one dimensional flow, Euler Equation takes the form,

$$\frac{\partial U}{\delta t}+\frac{\partial G}{\delta x}=0 \tag{13}$$

Where,

U (Vector of conserved variable) = $\begin{Bmatrix}\rho\\ \rho u\\ \rho e_m\end{Bmatrix}$

G (Flux vector) = $\begin{Bmatrix}\rho u\\ p+\rho u^2\\ (p+\rho e_m)u\end{Bmatrix}$

Also,

$$p+e=\rho\left(\frac{p}{\rho}+e_m\right)=\rho h_T \tag{14}$$

Where ρ is the density of the fluid

u is the velocity of the fluid

e_m is the energy per unit mass of the fluid

3 Numerical Schemes

3.1 Flux Vector Splitting (FVS) Schemes:

The basic concept of flux vector splitting method is to decompose the flux at the interface of one left and one right state, $G_{\frac{1}{2}}$ into two parts;

$$G_{\frac{1}{2}}=G_l^{+}+G_r^{-} \tag{15}$$

G^+ and G^- represents the contribution of the flux associated with the waves that moves from left to right and right to left respectively across the cell interface at half.

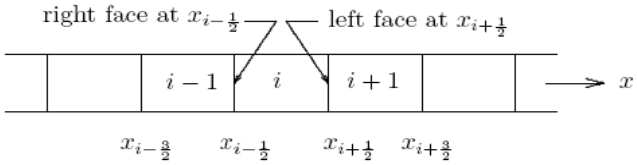

Fig.1. Flux splitting at the cell interface

There are many FVS schemes like Steger and Warming method [10], Van Leer algorithm etc. In our project, we have used the Van Leer's method which is elaborately discussed below.

3.1.1: Van Leer's Flux Vector Splitting:

Van Leer [8] provided the splitting by splitting the terms containing Mach Number in the flux Vector. The flux Vector can be expressed as function of Mach Number as:

$$G=\begin{bmatrix}G_1\\ G_2\\ G_3\end{bmatrix}=\begin{bmatrix}\rho aM\\ \frac{\rho a^2}{\gamma}\left(\gamma M^2+1\right)\\ \rho a^3M\left(\frac{1}{2}M^2+\frac{1}{\gamma-1}\right)\end{bmatrix} \tag{16}$$

Van Leer Split the Mach Number as,

$$M=M^{+}+M^{-} \tag{17}$$

Where,

$$M^{+}=\begin{cases}0, & M \le -1\\ \frac{1}{4}(M+1)^2, & -1<M<1\\ M, & M \ge 1\end{cases}$$

$$M^{-}=\begin{cases}M, & M \le -1\\ -\frac{1}{4}(M-1)^2, & -1<M<1\\ 0, & M \ge 1\end{cases}$$

The split fluxes are obtained in the following way:

$$G^{+}=\frac{\rho a}{4}(M+1)^2\begin{bmatrix}1\\ \frac{(\gamma-1)u+2a}{\gamma}\\ \frac{((\gamma-1)u+2a)^2}{2(\gamma+1)(\gamma-1)}\end{bmatrix}, \text{for } |M|<1 \tag{18}$$

And,

$$G^{-}=-\frac{\rho a}{4}(M-1)^2\begin{bmatrix}1\\ \frac{(\gamma-1)u-2a}{\gamma}\\ \frac{((\gamma-1)u-2a)^2}{2(\gamma+1)(\gamma-1)}\end{bmatrix}, \text{for } |M|<1 \tag{19}$$

Otherwise, $G^{+}=G,\ G^{-}=0$ for $M \ge 1$
And, $G^{+}=0,\ G^{-}=G$ for $M \le -1$

Van Leer further suggested that conventional flux vector splitting had certain limitations. One dissatisfaction with flux vector splitting is highly dissipative property of FVS schemes, which leads to diffused boundary layers in Navier-Stokes codes, diffused contact discontinuities and slip surfaces. This is in contrast to FDS such as Roe's Scheme. As a result, the attached boundary layers to be resolved by Navier Stokes codes using flux vector splitting get artificially broadened, and adiabatic wall temperature becomes inaccurate.

4 Reconstruction and Use of Limiters

4.1 Introduction:

The semi-discrete form of the Euler equations is

$$\frac{dU_i}{dt}+\frac{(G_{i+1/2}-G_{i-1/2})}{\Delta x}=0 \tag{20}$$

Where $U_i(t)$ the cell is averaged vector of dependent variables,

$$U_i(t)=\frac{1}{V_i}\int_{v_i} U dx dy \tag{21}$$

$G_{i\pm 1/2}$ = is the spatial flux quadrature

$$G_{i\pm 1/2}=\frac{1}{A_{i\pm 1/2}}\int_{x_{i\pm 1/2}} G_{\perp} dy \tag{22}$$

And $A_{i\pm 1/2}=\Delta y$ is the surface area of the face at $x_{i\pm 1/2}$. For a one-dimensional flow,

$$G_{i\pm 1/2}=U_{\perp_{i+1/2}}$$

Where $G_{\perp}$ is given by;

$$G_{\perp}=\begin{Bmatrix}U_2\\ \frac{U_2^2}{U_1}+(\gamma-1)\left(U_3-\frac{1}{2}\frac{U_2^2}{U_1}\right)\\ \frac{U_2U_3}{U_1}+(\gamma-1)\frac{U_2}{U_1}\left(U_3-\frac{1}{2}\frac{U_2^2}{U_1}\right)\end{Bmatrix} \tag{23}$$

The discretization of the domain and introduction of the volumeaveraged vector $U_i(t)$ result in a loss of information regarding $U(x,t)$. Consider, for example, the periodic function $U(x)=\sin x$ for $0 \le x \le 2\pi$. Assume ten cells are employed. The exact function $U(x)$ and cell averaged values U_i are shown in Fig. 4.1. Within a given cell, the cell averaged value is only an approximation of the exact function U. Of course, the approximation improves as the size of the cell is reduced.

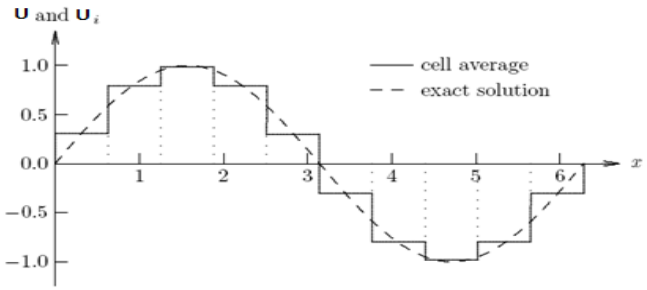

Fig.2. Flux splitting at the cell interface

The time evolution of U_i requires the flues, $G_{i\pm 1/2}$ which, in turn, must be computed using the U_i in the vicinity of $x_{i\pm 1/2}$. Within each cell i, a local approximate reconstruction $U_i(x)$ of the exact function $U(x)$ can be formed to compute the fluxes. Note, however, that discontinuity may exist at each cell interface, i.e., $U_i(x_{i+1/2}) \neq U_{i+1}(x_{i+1/2})$. The algorithm for the fluxes $G_{i\pm 1/2}$ must take this discontinuous behavior into consideration. The simplest reconstruction is, $U_i(x) = U_i$ which is first-

order accurate. This methodleads to excessive numerical diffusion, however, and is generally not acceptable. We therefore seek reconstruction methods of higher order accuracy. Three methods are presented in the following sections. U_i is the cell averaged values in cell *i* and is therefore a constant. $U_i(x)$ is a function defined in cell *i* that is in general not a constant. $U_i(x)$ is constructed to provide a closer approximation to $U(x)$ than is afforded by U_i.

4.2 Monotonic Upstream-centered Scheme for Conservation Laws (MUSCL):

.

Table 1: Reconstruction Table

K	Order	Definition
1	2nd	Centered
⅓	3rd	Upwind-biased
0	2nd	Upwind-biased
-1	2nd	Upwind

The MUSCL scheme is:

$$U^{l}_{i+½} = U_i + \frac{1}{4}\left[(1-\kappa)\Delta U_{i-½} + (1+\kappa)\Delta U_{i+½}\right] \quad (24)$$

$$U^{r}_{i-½} = U_i - \frac{1}{4}\left[(1-\kappa)\Delta U_{i+½} + (1+\kappa)\Delta U_{i-½}\right] \quad (25)$$

For κ=1

$$\Delta U_{i-½} = \Delta U_{i-½} \qquad \Delta U_{i+½} = \Delta U_{i+½} \quad (26)$$

For $\kappa = \frac{1}{3}$ with $\Delta U_{i+½} \geq 0$ and $\Delta U_{i-½} \geq 0$

$$\Delta U_{i-½} = \begin{cases} \Delta U_{i-½}, \text{ if } \Delta U_{i-½} \leq b\Delta U_{i+½} \\ b\Delta U_{i+½}, \text{ if } \Delta U_{i-½} > b\Delta U_{i+½} \end{cases} \quad (27)$$

$$\Delta U_{i+½} = \begin{cases} \Delta U_{i+½}, \text{ if } \Delta U_{i+½} \leq b\Delta U_{i-½} \\ b\Delta U_{i-½}, \text{ if } \Delta U_{i+½} > b\Delta U_{i-½} \end{cases} \quad (28)$$

For $\kappa = \frac{1}{3}$ with $\Delta U_{i+½} \geq 0$ and $\Delta U_{i-½} \leq 0$

$$\Delta U_{i-½} = \begin{cases} \Delta U_{i-½}, \text{ if } \Delta U_{i-½} \geq -2\Delta U_{i+½} \\ -2\Delta U_{i+½}, \text{ if } \Delta U_{i-½} < -2\Delta U_{i+½} \end{cases} \quad (29)$$

$$\Delta U_{i+½} = \begin{cases} \Delta U_{i+½}, \text{ if } \Delta U_{i+½} \leq -2\Delta U_{i+½} \\ -2\Delta U_{i-½}, \text{ if } \Delta U_{i+½} > -2\Delta U_{i+½} \end{cases} \quad (30)$$

For $\kappa = \frac{1}{3}$ with $\Delta U_{i+½} \leq 0$ and $\Delta U_{i-½} \leq 0$

$$\Delta U_{i-½} = \begin{cases} \Delta U_{i-½}, \text{ if } \Delta U_{i-½} \geq b\Delta U_{i+½} \\ b\Delta U_{i+½}, \text{ if } \Delta U_{i-½} < b\Delta U_{i+½} \end{cases} \quad (31)$$

$$\Delta U_{i+½} = \begin{cases} \Delta U_{i+½}, \text{ if } \Delta U_{i+½} \geq b\Delta U_{i-½} \\ b\Delta U_{i-½}, \text{ if } \Delta U_{i+½} < b\Delta U_{i-½} \end{cases} \quad (32)$$

For $\kappa = \frac{1}{3}$ with $\Delta U_{i+½} \leq 0$ and $\Delta U_{i-½} \geq 0$

$$\Delta U_{i-½} = \begin{cases} \Delta U_{i-½}, \text{ if } \Delta U_{i-½} \leq -2\Delta U_{i+½} \\ -2\Delta U_{i+½}, \text{ if } \Delta U_{i-½} > -2\Delta U_{i+½} \end{cases} \quad (33)$$

$$\Delta U_{i+½} = \begin{cases} \Delta U_{i+½}, \text{ if } \Delta U_{i+½} \leq -2\Delta U_{i-½} \\ -2\Delta U_{i-½}, \text{ if } \Delta U_{i+½} > -2\Delta U_{i-½} \end{cases} \quad (34)$$

For κ=0 and -1

$$\Delta U_{i-½} = \min \bmod\left(\Delta U_{i-½}, b\Delta U_{i+½}\right) \quad (35)$$

$$\Delta U_{i+½} = \min \bmod\left(b\Delta U_{i-½}, \Delta U_{i+½}\right) \quad (36)$$

Where

$$\min \bmod(x, y) = \begin{cases} x \text{ if } |x| \leq |y| \text{ where x and y have the same sign.} \\ y \text{ if } |x| > |y| \text{ where x and y have the same sign.} \\ 0 \text{ if x and y have opposite signs.} \end{cases}$$

4.3 Use of Limiter:

Second and higher order upwind spatial discretization's [5] require the use of so called *limiters* or *limiter functions* in order to prevent the generation of oscillations and spurious solutions in regions of high gradients (e.g., at shocks).The purpose of a limiter is to reduce the slopes (i.e., $\frac{U_{i+1} - U_i}{\Delta x}$) used to interpolate a flow variable to the face of a control volume, in order toconstrain the solution variations. At strong discontinuities, the limiter has toreduce slopes to zero to prevent the generation of a new extremum.The last requirement to be imposed on a limiteris quite obvious - the original unlimited discretization has to be obtained in smooth flow regions, in order to keep the amount of numerical dissipation **as**low as possible.

In our project work the following limiter functions have been used for the second order MUSCL scheme.

- Minmod Limiter Function.
- Van-Albada Limiter Function.

Minmod Limiter Function:

$$\Phi_{mm}(r) = \max\left[0, \min(1, r)\right];\ \lim_{r\to\infty} \Phi_{mm}(r) = 1 \tag{37}$$

This limiter is used for κ=-1, i.e. an upwind scheme

Van-Albada Limiter Function:

This limiter is used for forκ=0, i.e. an upwind-biased scheme. The expressions for the left and right states are:

$$U_r = U_{i+1} - \frac{1}{2}\delta_r \qquad U_l = U_i + \frac{1}{2}\delta_l \tag{38}$$

The function δ is formally identical for both the states.It reads

$$\delta = \frac{a(b^2+\varepsilon) + b(a^2+\varepsilon)}{a^2 + b^2 + 2\varepsilon} \tag{39}$$

The coefficient a and b are defined for the left and right states as

$$a_l = \Delta_+ U_i = U_{i+1} - U_i,\ \mathrm{b}_l = \Delta_- U_i = U_i - U_{i-1}$$

$$a_r = \Delta_+ U_{i+1} = U_{i+2} - U_{i+1}, b_r = \Delta_- U_{i+1} = U_{i+1} - U_i \tag{40}$$

5 Problem Statement

5.1 Sod's Shock tube problem:

The Shock Tube Problem [6] is a classical benchmark problem for numerical algorithms involving compressible flow, where study of generation and propagation of expansion and shock waves are to be understood. Our problem consists of a tube of 10 meters in length which is filled with air and separated by a diaphragm which represents the interface between two cells contain air at different pressure, density and velocity located at the middle of the tube. The state of the air on the left side of the diaphragm is different from that on the right side. This results in a discontinuous initial distribution.

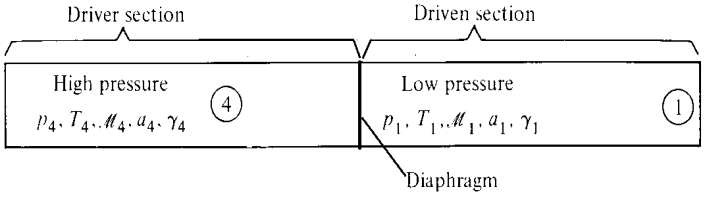

Fig.3. Driver and Driven Sections of a Shock Tube

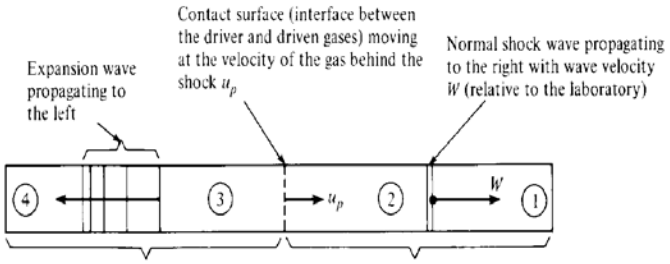

Fig.4. Schematic Layout of Shock Tube

In this paper, the distribution is chosen with the following initial condition:-

Length of the tube (L) = 10 m

Diaphragm Location = 5 m

Pressure on the driving side (P_4) =100000 Pa

Pressure on the driven side (P_1) =10000 Pa

Density on the driving side (ρ_4) = 1 $^{Kg}/_{m^3}$

Density on the driven side (ρ_1) = 0.125 $^{Kg}/_{m^3}$

Fluid velocity at the driving side (u_4) = 0 $^{m}/_{s}$

Fluid velocity at the driven side (u_1) = 0 $^{m}/_{s}$

given for left and right side of tube. The isentropic coefficient has been γ = 1.4. At time t=0 seconds, the diaphragm rupture and the air propagates in the tube. The flow parameters are recorded upto time t=0.0061 sec. According to Euler's equations during this propagation two discontinuities called shock and contact discontinuity arises. We discuss the impact of this result on the development of high-resolution shock-capturing numerical codes to solve the equations of relativistic hydrodynamics.

6 Results

6.1 Analytical:

The solution of the Riemann problem is found by solving an implicit algebraic equation which gives the pressure in the intermediate states. The solution presented here contains as a particular case the special relativistic shock-tube problem in which the gas is initially at rest. The above initial conditions are taken for solving the Sod's shock tube problem analytically. So, from the ideal gas equation,

$$P_1 = \rho_1 R T_1 \tag{41}$$
$$\Rightarrow T_1 = 278.7456 \text{ K}$$

$$P_4 = \rho_4 R T_4 \tag{42}$$
$$\Rightarrow T_4 = 348.432 \text{ K}$$

Again from,

$$a = \sqrt{\gamma R T} \tag{43}$$

$\Rightarrow a_1 = 334.664 \ {}^{m}/_{s}$

$\Rightarrow a_4 = 374.166 \ {}^{m}/_{s}$

Now,

$$\frac{P_4}{P_1} = \frac{P_2}{P_1}\left[1 - \frac{(\gamma-1)\left({}^{a_1}/_{a_4}\right)\left({}^{P_2}/_{P_1}-1\right)}{\sqrt{2\gamma}\sqrt{2\gamma+(\gamma+1)\left({}^{P_2}/_{P_1}-1\right)}}\right]^{-\frac{2\gamma}{(\gamma-1)}} \quad (44)$$

Across the expansion fan, the flow is isentropic, so

$\Rightarrow P_2 = P_3 = 30.314$ KPa

Across the expansion fan, the flow is isentropic, so

$$\rho_3 = \rho_4\left(\frac{P_3}{P_4}\right)^{\frac{1}{\gamma}} \quad (45)$$

$\Rightarrow \rho_3 = 0.42633 \ {}^{Kg}/_{m^3}$

And,

$$\rho_2 = \rho_1\left(\frac{1+\frac{(\gamma+1)}{(\gamma-1)}\left(\frac{P_2}{P_1}\right)}{\frac{(\gamma+1)}{(\gamma-1)}+\left(\frac{P_2}{P_1}\right)}\right) \quad (46)$$

$\Rightarrow \rho_2 = 0.26558 \ {}^{Kg}/_{m^3}$

Speed of shock wave,

$$U_{s_1} = u_4 - a_4\sqrt{\frac{(\gamma+1)}{2\gamma}\left(\frac{P^*}{P_4}-1\right)+1} = 554.09 \ {}^{m}/_{s} \quad (47)$$

Again,

$$T_3 = \frac{P_3}{R\rho_3} = 247.735 K$$

$$a_3 = \sqrt{\gamma R T_3} = 315.499 \ {}^{m}/_{s} \quad (48)$$

Similarly,

$T_2 = 397.71$ K

$a_2 = 399.749 \ {}^{m}/_{s}$

Velocity of the contact surface

$$U_c = u_4 - \frac{a_4}{\gamma}\left(\frac{P^*}{P_4}-1\right)\left[\frac{(\gamma+1)}{2\gamma}\left(\frac{P^*}{P_4}\right)+\frac{(\gamma-1)}{2\gamma}\right]^{-\frac{1}{2}} = 293.296 \ {}^{m}/_{s} \quad (49)$$

The velocity of the tail of the expansion fan $= u_p - a_3 = -22.209 \ {}^{m}/_{s}$

Within the expansion fan, the flow parameters at t=0.0061sec,

Location of the head of the expansion fan, $x = -a_4 \times t = -2.2824$ m

Location of the shock wave $= U_s \times t = 3.38$ m

6.2 Graphical:

Following are the graphical representations of analytical calculations for different parameters involved with the Riemaan Shock Tube problem. The parameters plotted against length of the tube are pressure, density, velocity, temperature and Mach number.

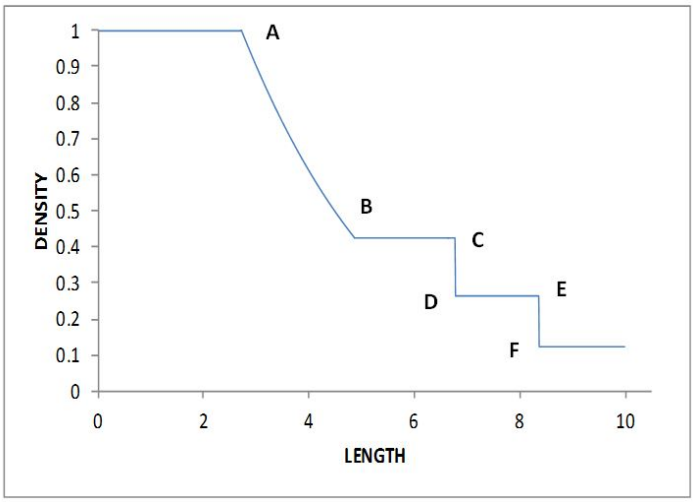

(a)

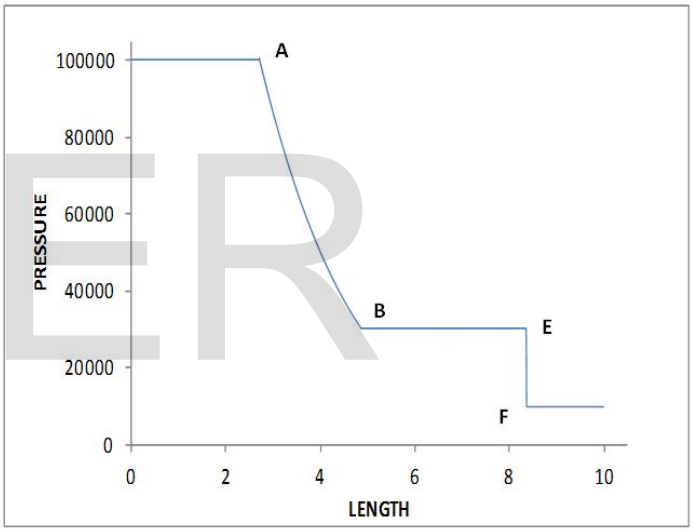

(b)

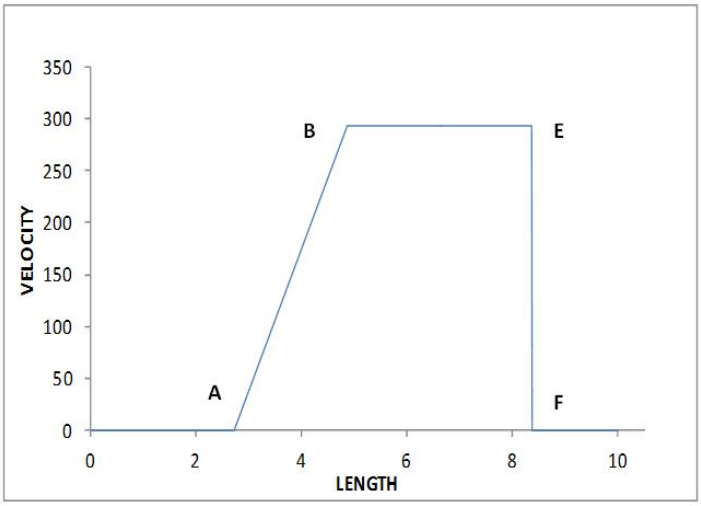

(c)

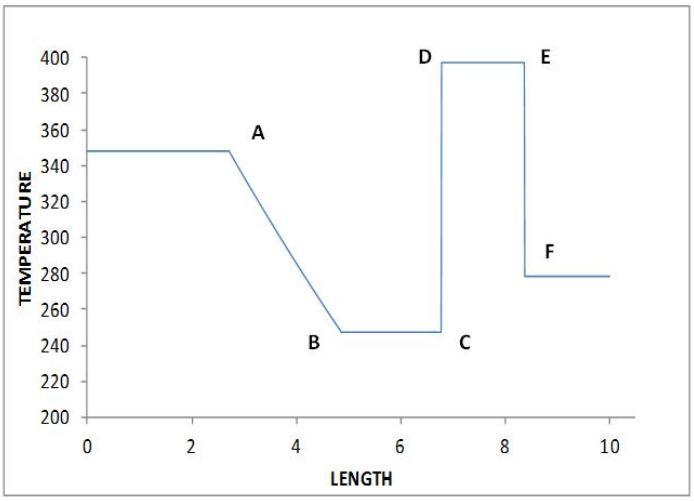

(d)

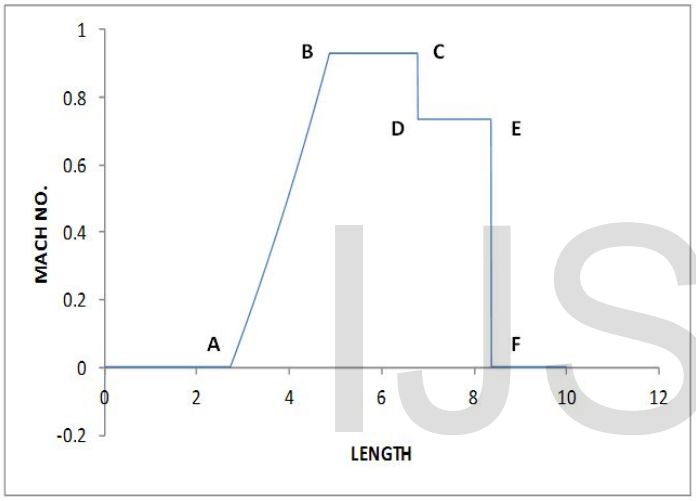

(e)

Fig.5. Variation of (a) Density, (b) Pressure, (c) Velocity, (d) Temperature and (e)Mach No. along the length of the Shock Tube

Here A and B represents the head and tail of expansion wave respectively. B to E represents the contact surface where B to C represents the left of the contact surface, point C o D represents the diffusive nature of the diaphragm and D to E represents the right of the contact surface. Point E to F represents the shock discontinuity. From the above figures, the variation of the conserved variables (density, pressure, velocity, temperature and Mach number) can be clearly seen.

6.3 Comparison of Van leer flux Splitting Scheme for different orders:

Van Leer's first, second and third order schemes are used to find the solution for the Riemann Shock tube problem. For higher order schemes, limiter functions like the Minmod and Van Albada are used to prevent the generation of oscillations and spurious solutions in regions of high gradients. A comparative study is also carried out between the results obtained from all the schemes and alongwith the analytical solution.

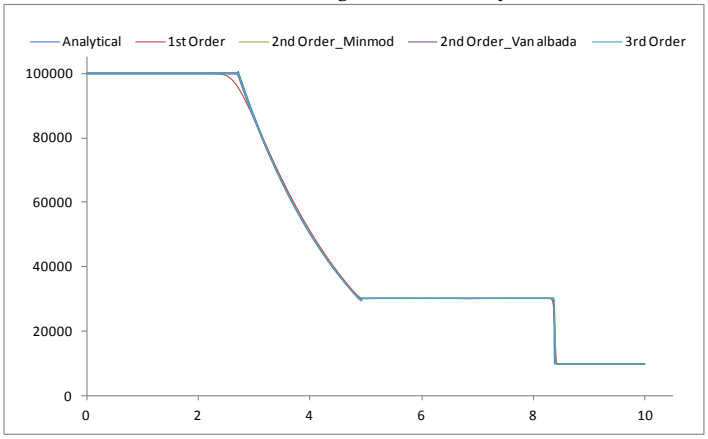

(a)

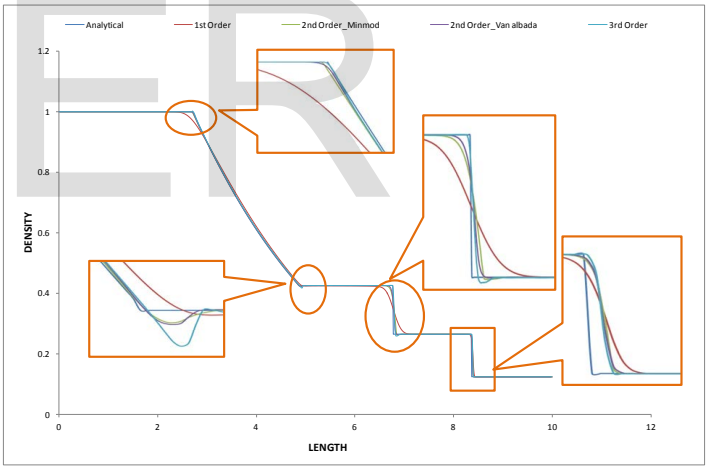

(b)

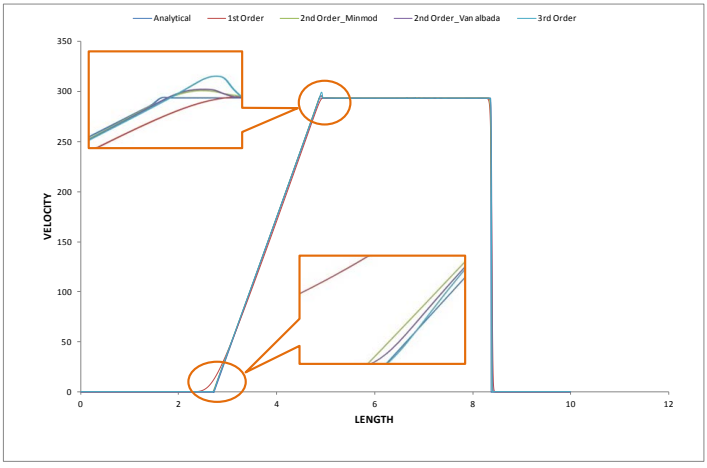

(c)

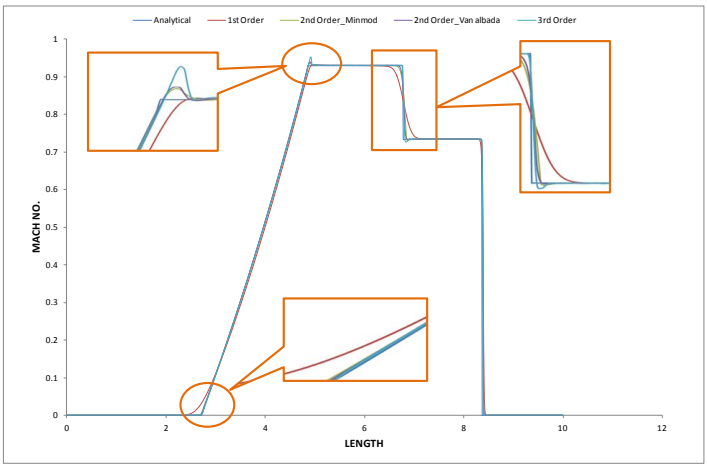

(d)

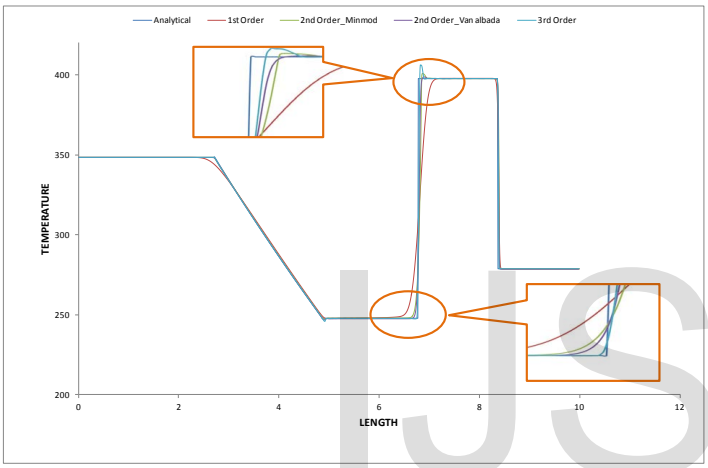

(e)

Fig.6. Comparison for (a) Pressure, (b) Density, (c) Velocity, (d) Mach No. and (e) Temperature along the length of the Shock Tube for Analytical, 1st order, 2nd order (Minmod), 2nd order (Van Albada) and 3rd order computations

Head of expansion wave at x = 2.72 m

x = 2.72 m	Pressure	Density	Velocity	Temperature	Mach No.
Analytical	99876.83	0.99912	0.329372	348.3094	0.00088
1st Order	95468.035	0.967469	2.524125	343.8262	0.033696
2nd Order Minmod	99127.1	0.9937625	2.351976	347.55805	0.0062945
2nd Order Van Albada	99394.29	0.9962179	1.636028	347.82595	0.0043765
3rd Order	99784.07	0.9984605	0.5855965	348.2156	0.0015655

Tail of expansion wave at x = 4.86 m

x = 4.86 m	Pressure	Density	Velocity	Temperature	Mach No.
Analytical	30313.012	0.426313	293.2863	247.7491	0.929569
1st Order	31055.01	0.433296	287.8655	249.72645	0.9087705
2nd Order Minmod	30438.555	0.427574	292.35565	248.04495	0.926066
2nd Order Van Albada	30443.145	0.4276445	292.321	248.0413	0.925963
3rd Order	30497.82	0.4281945	292.9155	248.136	0.924443

Contact Surface at x = 6.8 m

x = 6.8 m	Pressure	Density	Velocity	Temperature	Mach No.
Analytical	30313.02	0.265514	293.2863	397.706	0.733678
1st Order	30268.315	0.333145	293.533	316.591	0.8230235
2nd Order Minmod	30313.755	0.339086	293.30955	311.6517	0.8290295
2nd Order Van Albada	30284.815	0.318724	293.3459	331.63005	0.8041145
3rd Order	30301.44	0.299428	293.39925	353.6529	0.779201

Shock wave at x = 8.38 m

x = 8.38 m	Pressure	Density	Velocity	Temperature	Mach No.
Analytical	10000	0.125	0	278.7456	0
1st Order	21265.58	0.207143	203.582	356.94845	0.536731
2nd Order Minmod	22066.58	0.211982	206.9611	360.5405	0.5415365
2nd Order Van Albada	21400.47	0.207076	198.615	356.6211	0.520856
3rd Order	20945.62	0.2029355	188.11205	353.8005	0.4918805

There are many effects for using the higher order schemes as they are very prone to in stability and oscillations in the vicinity of discontinuity. This effect is very well rectified by the use of limiters. Moreover, the higher order schemes give far better and accurate solutions than lower order schemes. As the order of the scheme is increased, the numerical dissipation is reduced. From the graphs seen above, it is seen that the third order solution is in better agreement with the analytical solution than the second order solution which in turn is better than the first order solution. The highly dissipative nature of first order solution is quite evident in the smeared shock and contact discontinuities.

For higher order schemes, reconstruction methods are used to increase the accuracy of the solution obtained.

Conclusion

This work is carried out using basic schemes for numerical solution of compressible flow problems so that in future more challenging problems in CFD can be encountered. The various schemes for numerical solution of One Dimensional Flow is studied. The Van leer Flux Vector Scheme is used for numerical simulation of the Sod's Shock Tube. For the purpose of numerical simulation, a C code is developed.

Based on our study following conclusions can be made:

1) The results of the Van Leer's third order solution for Sod's shock tube problem are found in excellent agreement with the analytical solution. Hence the Code is validated.
2) In Sod's shock tube problem, the accuracy of the third order solution is much better than that of first and second order solutions. This is quite evident at the smeared shock

and contact discontinuities where the dissipative nature of the first and second order solution is clearly seen.

3) Following the trend the results obtained from higher order methods are expected to be more accurate than the preceding orders.
4) The computer simulation is found to be an economic approach as compared to the experimental approach. Furthermore, it is free of some of the constraints imposed on the experimental method for obtaining information upon which to base a design such as the difficulty faced in physical simulation of the operating environment. The only difficulty in computational approach lies in mathematically modeling the complex physical phenomena.

References

1. John D. Anderson, Jr., Computational Fluid Dynamics (The Basic with Application), McGraw Hill Inc., 1995
2. John C. Tennehill, Dale A. Anderson and Richard H. Pletcher, Computational Fluid Mechanics and Heat Transfer, Taylor and Francis, 1997
3. John D. Anderson, Jr., Modern Compressible Flow, McGraw Hill Book Company, 1982
4. Doyle D. Knight, Elements of numerical methods for compressible flow, Cambridge University Press, 2006
5. J. Blazek, Computational Fluid Dynamics: Principles and Applications.
6. G. A. Sod, A Survey of Several Finite Difference Methods for Systems of Non-linear Hyperbolic Conservation Laws, Journal of Computational Physics, 27, 1978, 1-31
7. B. van Leer, Towards the Ultimate Conservative Difference Scheme IV. A New Approach to Numerical Convection, Journal of Computational Physics, 23, 1977, 276-299
8. B. van Leer, Towards the Ultimate Conservative Difference Scheme V. A Second Order Sequel to Godunov Method, Journal of Computational Physics, 32, 1979, 101-136.
9. P.L. Roe, Approximate Riemann solvers, parameter vectors and difference schemes, Journal of Computational Physics 43, 1981, 357–372
10. J. L. Steger and R. F. Warming, Flux Vector Splitting of the Inviscid Gas Dynamic Equations with Application to Finite-Difference Methods, Journal of Computational Physics. 40,1981, 263-293
11. B. van Leer, Flux vector splitting for Euler equations, Lecture Notes in Physics, 170 ,1982, 507-519
12. S. Jaisankar and S.V. Raghurama Rao, Diffusion regulation for Euler Solvers, Journal of Computational Physics, 221 (2007) 577-599
13. S. Jaisankar and T.S. Sheshadri, Directional Diffusion Regulator (DDR) for some numerical solvers of hyperbolic conservation laws, Journal of Computational Physics, 233(2013) 83-89.
14. Anil Kapahi and Chao-Tsung Hsiao, A multi-material flow solver for high speed compressible flows, Computers and Fluids, 115 (2015) 25-45.

- *Mohammad Asif Sultan is currently pursuing masters degree in Automobile Engineering in National Institute of Technology Warangal, India, Ph: +91-7407813499. Email id: asifsltn@gmail.com*
- *Manash Jyoti Konwar is currently pursuing masters degree in Automobile Engineering in National Institute of Technology Warangal, India, Ph: +91-7578095432, Email id: rickykonwar@gmail.com*